Journal of Non-Crystalline Solids 355 (2009) 1489–1495

Contents lists available at ScienceDirect

Journal of Non-Crystalline Solids

journal homepage: www.elsevier.com/locate/jnoncrysol

Optical properties of Ge–Se–Te wedge-shaped films by using only transmission spectra

K.A. Aly *

Department of Physics, Faculty of Science, Al Azhar University, Assiut, Egypt

ARTICLE INFO

Article history:
Received 31 March 2008
Received in revised form 20 April 2009
Available online 21 June 2009

PACS:
77.55.+f
71.23.Cq
71.55.Jv
71.15.Nc

Keywords:
III–V semiconductors
X-ray diffraction
Band structure
Chalcogenides
Optical spectroscopy
Tellurites

ABSTRACT

Amorphous $Ge_{10}Se_{90-x}Te_x$ (with $x = 0$, 5, 10 and 15 at.%) thin films were prepared by thermal evaporation method. The optical transmission spectra of these films were measured in the wavelength range of 500–2500 nm in order to drive the refractive index and the absorption coefficient of these films. Applying the analytical expressions proposed by Swanepoel, enabling the calculations of optical constants of thin films with non-uniform thickness with high accuracy. Furthermore, the dispersion of the refractive index is discussed in terms of the single-oscillator Wemple and DiDomenico model. It was found that, the mechanism of the optical absorption follows the rule of the allowed non-direct transition. The optical band gab, E_g, and the oscillator energy, E_o, decrease while the dispersion energy, E_d, increases by increasing Te content. The relationship between the obtained results and the chemical compositions of the $Ge_{10}Se_{90-x}Te_x$ thin films were discussed in terms of the chemical bond approach, the excess of Se–Se homopolar bonds and the cohesive energy (CE).

1. Introduction

Chalcogenide semiconducting glasses have received great attention because of their important optical applications in the infrared region [1,2] due to their high transmittance in the IR spectral region [3]. The common feature of these glasses is the presence of localized state in the mobility gap as a result of the absence of long-range order as well as various inherent defects. Investigation of electron transport in disordered systems has been gradually developed and the investigation of gap states is of particular interest because of their effect on the electrical properties of semiconductors [4]. A number of papers [5–11] have appeared in the literature reporting the electrical and photoelectrical properties, glass formation, and crystallization kinetics of Ge–Se–Te glasses, allowing the use of these materials in the fabrication of a great number of optical devices [12–14]. The accurate determination of the optical constants of these materials is important in order to exploit and develop their interesting technological applications. The optical characterization of thin films often requires the use of highly refined computer numerical techniques applied to both optical transmission and reflection spectra [15–18]. In contrast, a relatively simple and straightforward method for determining the optical constants, using only their transmission spectra, has been proposed by Swanepoel [19,20], which is also particularly useful because it accounts for a possible lack of film-thickness uniformity. This method is based on the upper and lower envelopes of normal-incidence optical transmission spectra. It takes into account the spectrum compression (i.e., increase of minima and decrease of maxima of interference caused by film-thickness) variations across the light spot defined by the spectrophotometer beam. Since the samples being the object of the present study were thin films with relatively non-uniform thicknesses, said method was successfully applied. The samples were layers of a ternary amorphous materials having a chemical composition $Ge_{10}Se_{90-x}Te_x$ (with $x = 0$, 5, 10 and 15 at.%) deposited onto cleaned glass substrates by vacuum thermal evaporation. Accurate values for the optical constants such as refractive index, the extinction coefficient and film-thickness were obtained and discussed.

2. Experimental details

Different compositions of the $Ge_{10}Se_{90-x}Te_x$ (with $x = 0$, 5, 10 and 15 at.%) chalcogenide glasses were prepared from Ge, Se, and Te elements with high purity (5 N) by the usual melt quench technique. Materials were weighed according to their atomic percentages,

* Tel./fax: +2 0882181436.
E-mail address: kamalaly2001@Gmail.com

0022-3093/$ - see front matter © 2009 Elsevier B.V. All rights reserved.
doi:10.1016/j.jnoncrysol.2009.05.042

charged into cleaned silica tubes then sealed under vacuum of $\approx 1.33 \times 10^{-3}$ Pa the ampoules were put into a furnace at around 1300 K for 24 h. During the heating process the ampoules were shaken several times to maintain their uniformity, and then the ampoules were quenched in ice cooled water to avoid the crystallization. Thin films were prepared by thermal evaporation of small ingot pieces onto electronically cleaned glass substrates (microscope slides). The thermal evaporation process was performed by using a coating (Denton Vacuum 502 A) system, at a pressure of approximately 1.33×10^{-3} Pa, during the deposition process. The thickness of the film was determined using a quartz crystal monitor (Denton's model DTM-100). The rate of the film deposition was controlled using the same DTM-100 quartz crystal monitor and it was 1–10 Å/s. Chemical compositions of the chalcogenide films were found to be $Ge_{10\pm0.09}Se_{90\pm0.7}$, $Ge_{10\pm0.1}Se_{85\pm0.8}Te_{5\pm0.04}Ge_{10\pm0.07}Se_{80\pm0.7}Te_{10\pm0.08}$ and $Ge_{10\pm0.08}Se_{75\pm0.8}Te_{15\pm0.13}$ on the basis of electron microprobe X-ray analysis, using a (Link Analytical Edx) scanning electron microscope. The deviations in the elemental compositions of the evaporated thin films from their initial bulk specimens does not exceed than ±1 at.%. The amorphous state of these materials was checked using X-ray (Philips type 1710 with Cu as a target and Ni as a filter, $\lambda = 1.5418$ Å) diffractometer. The absence of crystalline peaks confirms the glassy state of the prepared samples.

Optical transmittance for $Ge_{10}Se_{90-x}Te_x$ thin films has been measured using a double beam (Shimadzu 2101 UV–VIS) computer controlled spectrophotometer, at normal incidence of light and in the wavelength range 500–2500 nm. The accuracy to which, λ, can be measured is ±1 nm. Without a glass substrate in the reference beam, the measured transmittance spectra were used to calculate the refractive index and the average film-thickness of different compositions of $Ge_{10}Se_{90-x}Te_x$ thin films.

3. Theoretical considerations

According to [19,20] one can write or use the expression of the transmission spectra at normal incidence for homogeneous film with uniform thickness d and complex refractive index $n_c = n - ik$, or absorption coefficient α on transparent substrate with refractive index s. The substrate is considered to be perfectly smooth, but thick enough so that in practice the planes are not perfectly parallel so that all interference effects due to the substrate are destroyed. The substrate–film system is surrounded by air with refractive index $n_o = 1$. Considering all the multiple reflections at the three interfaces into account, it is noted in the case $k^2 \ll n^2$ that the expression for the transmittance T at normal incidence is written as well as written before by [19,20]:

$$T = \frac{Ax_a}{B - Cx_a\cos(\phi) + Dx_a^2}, \tag{1}$$

where $A = 16n^2s$, $B = (n+1)^3(n+s^2)$, $C = 2(n^2-1)(n^2-s^2)$, $D = (n-1)^3(n-s^2)$, $\phi = 4\pi n\bar{d}/\lambda$, $x_a = \exp(-\alpha d)$ and $k = \alpha\lambda/4\pi$. The two envelops around the interference maxima, T_{Mo}, and minima, T_{mo}, can be expressed as continuous function of λ by:

$$T_{Mo}, T_{mo} = \frac{Ax_a}{B \mp Cx_a + Dx_a^2}, \tag{2}$$

where $-$ in the $\mp$ refers to T_{Mo} and $+$ to T_{mo}.

The optical characterization method considered in this work that assumes the film-thickness varies linearly over the illuminated area by Δd i.e $d = d \pm \Delta d$ as observed before by Màrquez et al. [21] (see Fig. 1). The expression for the transmittance $T_{\Delta d}$ spectra in this case is given by integrating Eq. (1) over both Δd and x [20] but, this is prohibitively difficult analytically, and an approximation is to consider x to have an average value, $\bar{x} = \exp(-\alpha\bar{d})$ over the range of integration with respect to Δd. This approximation is an excellent one provided $\Delta d \ll d$. Thus, the transmittance $T_{\Delta d}$ can be expressed as [21,22]:

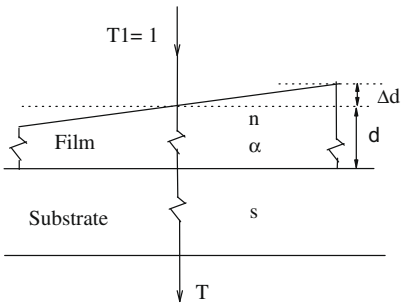

Fig. 1. Schematic diagram for an absorbing thin film with non-uniform film-thickness ($d \pm \Delta d$) on a thick finite transparent substrate [25].

$$T_{\Delta d} = \frac{1}{\phi_2 - \phi_1}\int_{\phi_1}^{\phi_2} \frac{A\bar{x}}{B - C\bar{x} + D\bar{x}^2}, \tag{3}$$

where $\phi_1 = 2\pi n(\bar{d} - \Delta d)$ and $\phi_2 = 2\pi n(\bar{d} + \Delta d)$.

The integral yields [21,22]:

$$T_{\Delta d} = \frac{\lambda \cdot a}{4 \cdot \pi \cdot n \cdot \Delta d(1-b^2)^{1/2}}\left[\tan^{-1}\left(\frac{1+b}{(1-b^2)^{1/2}}\tan\frac{\phi_2}{2}\right) - \tan^{-1}\left(\frac{1+b}{(1-b^2)^{1/2}}\tan\frac{\phi_1}{2}\right)\right], \tag{4}$$

where

$$a = \frac{A\bar{x}}{B + D\bar{x}^2}, \quad b = \frac{C\bar{x}}{B + D\bar{x}^2}, \tag{5}$$

Furthermore, the expressions of the envelopes around the interference maxima and minima of the transmission spectrum can be written as [21,22]:

$$T_{M\bar{x}}, T_{m\bar{x}} = \frac{\lambda \cdot a}{4 \cdot \pi \cdot n \cdot \Delta d(1-b^2)^{1/2}}\left[\tan^{-1}\left(\frac{1 \pm b}{(1-b^2)^{1/2}}\tan\frac{\phi}{2}\right)\right], \tag{6}$$

where **+** in the $\pm$ refers to $T_{M\bar{x}}$ and $-$ to $T_{m\bar{x}}$. Substituting Eqs. (5) into (6) the following compact relation between the experimental envelopes T_M and T_m of the non-uniform film and the envelopes T_{Mo} and T_{mo} of the uniform film, with the same optical constants of the non-uniform film, are obtained [21,22]:

$$T_{M,m} = \frac{(T_{Mo}T_{mo})}{\phi}\tan^{-1}\left[\left(\frac{T_{Mo}}{T_{mo}}\right)^{\pm\frac{1}{2}}\tan\phi\right], \tag{7}$$

where + in the $\pm$ refers to T_M and $-$ to T_{mo}. The validity range of Eq. (7) is

$$\phi = 2\pi n\Delta d/\lambda, \quad 0 < \phi < \pi/2 \quad \text{or} \quad 0 < \Delta d < \lambda/4n. \tag{8}$$

After the known of the two envelopes, T_M and T_m, the two expressions included in Eq. (7) are two independent transcendental equations for T_{Mo}, T_{mo} and ϕ. Considering that, in the transparent region $T_{Mo} = T_s$, where T_s is the transmission of the substrate alone, the two expressions in Eq. (7) can be solved for T_{mo} and ϕ in this particular spectral region, using a rapidly-converging algorithm (Newton–Raphson iteration [21] or using mathcad 2000 professional program). Furthermore, it's necessary to tacking into account the well-known equation for the interference fringes, which due to the optical absorption, is verified at the tangent points,

$$2nd = m\lambda, \tag{9}$$

where m is the order number, in order to calculate T_{Mo} and T_{mo} over the whole spectral range under study, Eq. (9) can be rewritten as [19,20]:

$$\frac{l}{2} = \frac{2n\bar{d}}{\lambda} - m_1, \tag{10}$$

where $l = 0, 1, 2, 3, \ldots$ for the successive tangent points starting from the long-wavelength end, and m_1 is the order number of the first ($l = 0$) tangent point considered, while m_1 is an integer or a half-integer, for the upper or lower tangent points, respectively. Substituting Eq. (8) into (10) gives [21]:

$$\frac{l}{2} = \frac{\bar{d}}{\pi\Delta d}\phi - m_1, \tag{11}$$

where a straight line between $l/2$ and ϕ in the transparent region with slope yields $\bar{d}/(\pi\Delta d)$ that allows the determination of Δd and intercept m_1. Eq. (11) can be used for the calculation of ϕ for the tangent points in the region of absorption then, T_{Mo} and T_{mo} can be calculated through solving Eq. (7). Where, the values of T_{Mo} and T_{mo} are known, one can optically characterize the non-uniform chalcogenide films by the applying the procedure corresponding to uniform film [19–28].

After knowing T_{Mo} and T_{mo} the real part of the refractive index n can now be calculated at any wavelength in the medium and weak absorption region using the formula suggested by Swanepoel [19,20]:

$$n = [N + (N^2 - s^2)^{\frac{1}{2}}]^{\frac{1}{2}}, \tag{12}$$

where

$$N = 2s\frac{T_{Mo} - T_{mo}}{T_{Mo}T_{mo}} + \frac{s^2 + 1}{2}. \tag{13}$$

It was worth mentioned that, this formulae are valid only for films with uniform thickness and the two Eqs. (2) and (12) are not valid for films with non-uniform thickness [19,20]. The refractive index of the substrate s can be expressed as a continues function of wavelength through the suggested formula by Swanepoel [19,20] as:

$$s = \frac{1}{T_s} + \left(\frac{1}{T_s^2} - 1\right)^{\frac{1}{2}}. \tag{14}$$

Further more, the first approximate value of the film-thickness d_1 can be written in the following form [19,20]:

$$d_1 = \frac{\lambda_1 \cdot \lambda_2}{2 \cdot (n_{c2}\lambda_1 - n_{c1} \cdot \lambda_2)}, \tag{15}$$

where n_{c1} and n_{c2} are the refractive indices at two adjacent maxima (or minima) at λ_1, and λ_2, respectively, on the other side, the 'order' of a given extreme m, can be estimated from the above-mentioned basic equation for interference fringes $2nd = m\lambda$ using the average value of d_1 ($\bar{d}_1$), and the corresponding n_1. The calculation of the next thickness approximation d_2 is carried out via the interference condition, where n and m are now used. The average value of d_2 ($\bar{d}_2$) is the final calculated film-thickness. After that, substituting $\bar{d}_2$ and m again in the interference condition, the final value of the refractive index n_2 is obtained for each extreme.

For determining the extinction coefficient, k, Swanepoel [19,20] suggested that, in case of the uniform films thickness, the T_{Mo} curve be used over the whole range of the spectrum (the regions of strong, medium and weak absorption). The corresponding expression for calculating the absorbance x is as follows [19,20]:

$$x = \frac{E_{Mo} - [E_{Mo}^2 - (n^2 - 1)^3(n^2 - s^4)]^{\frac{1}{2}}}{(n-1)^3(n - s^2)}, \tag{16}$$

where

$$E_{Mo} = \frac{8n^2 s}{T_{Mo}} + (n^2 - 1)(n^2 - s^2),$$

then the absorption coefficient $\alpha(\lambda)$ can be calculated, using the well known expression $\alpha = \frac{-1}{d}\ln(x)$ [19]. When $\alpha(\lambda)$ is known the extinction coefficient k(λ) also can be determined by using the expression ($k = \alpha\lambda/4\pi$), which completes the derivation of all optical constants.

4. Results

The typical experimental transmission spectrum shown in Fig. 2(a) corresponds to $Ge_{10}Se_{90}$ wedge-shaped thin films as an example. The transmission of the substrate alone is shown as, T_s. The Two envelopes, T_M, and, T_m, are drawn around the extreme of each transmission spectrum using the Origin version 7 (Origin Lab Corp.) program, the maximum absolute accuracy of T_M and T_m is ±0:001. The obtained values of, T_M, and, T_m, are listed in Table 1. Using Eq. (7) the values of T_{Mo}, T_{mo}, and the first approximation of ϕ at each extrema of spectrum can be derived as shown in Table 1. The values of ϕ are shown in Table 1 as ϕ_1. Fig. 2(b) investigates the compositional dependence of the measured transmittance specter $Ge_{10}Se_{90-x}Te_x$ thin films. From this figure one can note that the addition of Te atoms at the expense of Se atoms sifts the transmittance spectra to the long wavelength side, i.e. low energy.

Fig. 3 represents the plots of l/2 versus ϕ_1 for $Ge_{10}Se_{90-x}Te_x$ thin films, the best straight lines through the points of the transparent region are drawn; the values of the correlation coefficient R corresponding to the least-squares fit for these data are 0.999. The deviations of the points for larger ϕ_1, from these straight lines indicate the onset of absorption, and these points must be rejected. Using the values of slope and intercept of Fig. 3, Eq. (11) can be rewritten for $Ge_{10}Se_{90-x}Te_x$ films with $x = 0$, 5, 10 and 15 at.% in the following form:

$$\frac{l}{2} = 7.21\phi_1 - 2.51, \tag{17a}$$

$$\frac{l}{2} = 6.35\phi_1 - 2.47, \tag{17b}$$

$$\frac{l}{2} = 8.76\phi_1 - 2.51, \tag{17c}$$

$$\frac{l}{2} = 5.89\phi_1 - 2.54. \tag{17d}$$

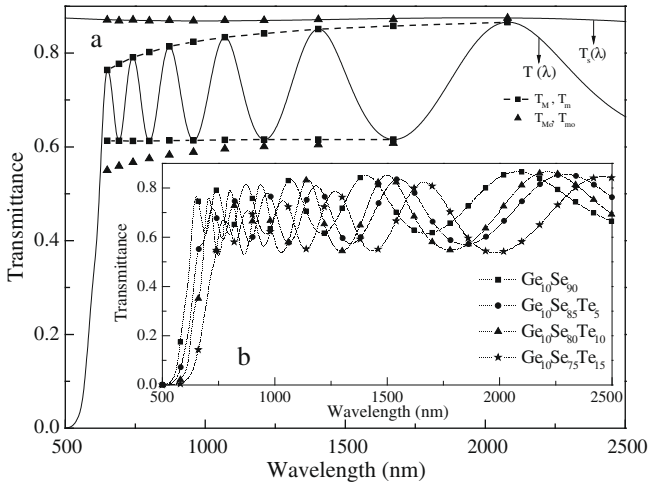

Fig. 2. (a) Transmission spectra, $T(\lambda)$ of the wedge-shaped $Ge_{10}Se_{90}$ thin film deposited onto thick transparent substrates. The T_{Mo}, T_M, T_m and T_{mo} defined in the text and $T_s(\lambda)$ is the transmission of the substrate alone. (b) Transmission spectra, $T(\lambda)$, of the wedge-shaped $Ge_{10}Se_{90-x}Te_x$ thin films.

Table 1
Values of λ, T_M, and T_m for $Ge_{10}Se_{90-x}Te_x$ thin films from transmission spectra of Fig. 2. The underlined values of transmittance are those given in the transmittance spectra of Fig. 2 and the others are calculated by the envelope method. Calculation of T_{Mo} and T_{mo} using T_M and T_m, then, the optical method for uniform films is used. It is worth noting that the exact value of m_1 as well as those obtained by Eq. 17(a–d).

Sample	λ ±1 nm	T_M ±0.001	T_m ±0.001	ϕ_1 ±0.001	T_{Mo} ±0.001	T_{mo} ±0.001	ϕ_2 ±0.001	n_1 ±0.001	d_1	m	d_2	n_2 ±0.001
$Ge_{10}Se_{90}$	1676	0.858	0.616	0.364	0.872	0.608	0.347	2.637		2.5	794	2.652
	1398	0.851	0.616	0.411	0.872	0.605	0.416	2.659		3	788	2.654
	1204	0.842	0.616	0.486	0.870	0.601	0.486	2.678	768	3.5	787	2.667
	1064	0.834	0.615	0.551	0.870	0.596	0.556	2.700	787	4	788	2.694
	962	0.824	0.614	0.622	0.869	0.589	0.625	2.725	822	4.5	794	2.74
	874	0.814	0.614	0.690	0.870	0.583	0.695	2.750	823	5	795	2.766
	794	0.802	0.613	0.766	0.869	0.575	0.765	2.776	754	5.5	787	2.764
	738	0.791	0.613	0.830	0.871	0.567	0.834	2.808	758	6	789	2.803
	688	0.777	0.613	0.909	0.869	0.559	0.904	2.833	803	6.5	789	2.830
	644	0.764	0.613	0.976	0.871	0.55	0.974	2.870	768	7	785	2.853
$\bar{d}_1 = 785$, $\delta_1 = 28$ nm (3.5%); $\bar{d}_2 = 790$, $\delta_1 = 4$ nm (0.51%)												
$Ge_{10}Se_{85}Te_5$	1844	0.85	0.574	0.411	0.872	0.564	0.387	2.799		2.5	823	2.807
	1550	0.841	0.575	0.467	0.873	0.56	0.466	2.827		3	822	2.831
	1340	0.83	0.576	0.535	0.873	0.556	0.545	2.852	819	3.5	822	2.856
	1184	0.815	0.576	0.624	0.869	0.55	0.624	2.876	827	4	823	2.884
	1062	0.805	0.577	0.682	0.874	0.543	0.703	2.915	811	4.5	820	2.910
	966	0.786	0.578	0.784	0.868	0.536	0.782	2.935	820	5	823	2.941
	888	0.773	0.579	0.853	0.872	0.527	0.861	2.979	820	5.5	820	2.974
	824	0.755	0.582	0.944	0.867	0.52	0.940	2.999	831	6	824	3.010
	770	0.736	0.585	1.031	0.864	0.512	1.019	3.028	865	6.5	826	3.047
	722	0.721	0.585	1.097	0.871	0.498	1.098	3.099	766	7	815	3.077
$\bar{d}_1 = 819 \pm 27$ nm (3.3%); $\bar{d}_2 = 822 \pm 2.97$ nm (0.36%)												
$Ge_{10}Se_{80}Te_{10}$	1774	0.859	0.548	0.304	0.873	0.542	0.286	2.899		2.5	765	2.887
	1490	0.853	0.546	0.341	0.873	0.538	0.343	2.915		3	766	2.910
	1298	0.844	0.544	0.395	0.871	0.533	0.400	2.942	790	3.5	772	2.958
	1140	0.834	0.54	0.454	0.870	0.525	0.457	2.979	761	4	765	2.969
	1024	0.825	0.538	0.509	0.870	0.519	0.514	3.001	748	4.5	767	3.000
	942	0.814	0.534	0.569	0.869	0.511	0.576	3.043	810	5	774	3.066
	864	0.805	0.531	0.614	0.873	0.503	0.629	3.067	813	5.5	775	3.094
	798	0.789	0.528	0.689	0.869	0.494	0.688	3.120	736	6	767	3.117
	746	0.775	0.525	0.749	0.868	0.485	0.743	3.165	721	6.5	766	3.157
	698	0.760	0.522	0.807	0.868	0.475	0.800	3.213	721	7	760	3.181
$\bar{d}_1 = 762 \pm 38$ nm (4.9%); $\bar{d}_2 = 768 \pm 4.6$ nm (0.6%)												
$Ge_{10}Se_{75}Te_{15}$	1978	0.840	0.541	0.453	0.871	0.528	0.429	2.944		2.5	840	2.960
	1664	0.831	0.544	0.509	0.875	0.525	0.515	2.970		3	840	2.988
	1438	0.815	0.545	0.590	0.874	0.519	0.600	3.004	832	3.5	838	3.013
	1270	0.798	0.547	0.678	0.872	0.513	0.685	3.034	827	4	837	3.041
	1140	0.780	0.550	0.766	0.871	0.501	0.771	3.091	804	4.5	830	3.07
	1038	0.762	0.553	0.852	0.870	0.5	0.856	3.096	843	5	838	3.107
	954	0.740	0.557	0.953	0.864	0.493	0.942	3.119	896	5.5	841	3.141
	884	0.724	0.562	1.028	0.869	0.484	1.027	3.168	831	6	837	3.175
	826	0.705	0.568	1.114	0.869	0.475	1.113	3.210	811	6.5	836	3.214
	772	0.686	0.570	1.191	0.876	0.46	1.198	3.292	735	7	821	3.235
$\bar{d}_1 = 822 \pm 45$ nm (5.46%); $\bar{d}_2 = 836 \pm 6$ nm (0.72%)												

The value of ϕ_2 at each extreme is now calculated from the expressions which result from modifying these last four equations, in such a way, the value of m_1 shown in each expression is appropriately rounded. The resulting exact value is the same namely (2) for $Ge_{10}Se_{90-x}Te_x$ thin films. The new values of ϕ for uniform films are shown in Table 1 by ϕ_2, using these values of ϕ_2, together with the values of, T_M, T_m, to drive the T_{Mo} and T_{mo} values by using Eq. (7). Values of T_{Mo} and T_{mo} are listed in Table 1. Knowing the values of the two envelopes T_{Mo} and T_{mo} helped us to apply Swanepoel method [19–28] in order to complete to drive all the optical constants as well detailed in the pervious section. The average value of film-thickness $\bar{d}$ for $Ge_{10}Se_{90-x}Te_x$ films are listed in Table 1 as $\bar{d}_1$ for the first approximation and $\bar{d}_2$ for the final value of the film-thickness with high accuracies of the final value of the average thickness $\bar{d}_2$ are 0.51%, 0.36%, 0.60% and 0.72% for $x = 0$, 5, 10 and 15, respectively. Substituting the values of $\bar{d}$ in to Eq. (11) and using the values of the slope in Eqs. (17a–d), then the values of Δd are obtained (Fig. 3). It is generally observed that, the higher average thickness is the higher the thickness variation as well as worth mentioned before [20,21]. The final values of the refractive index n_2 can be fitted to a reasonable function such as the two-term Cauchy dispersion relationship, $n(\lambda) = a + b/\lambda^2$ which can be used for extrapolating the whole wavelengths [29] (see solid lines in Fig. 4). The least-squares fit of the four sets of n_2 values for different composition samples listed in Table 1, yields $n = 2.597 + 1.16 \times 10^5/\lambda^2$ for $Ge_{10}Se_{90}$ sample, $n = 2.76 + 1.68 \times 10^5/\lambda^2$ for $Ge_{10}Se_{85}Te_5$ sample, $n = 2.84 + 1.74 \times 10^5/\lambda^2$ for $Ge_{10}Se_{80}Te_{70}$ and $n = 2.91 + 1.98 \times 10^5/\lambda^2$ $Ge_{10}Se_{75}Te_{15}$ thin films where the regression coefficient of the least-squares fitting written in Fig. 4.

The energy dependence of, n, for amorphous materials can be fitted according to the well known single-oscillator model (WDD) [30]:

$$n^2(h\nu) = 1 + \frac{E_0 \cdot E_d}{E_0^2 - (h\nu)^2}, \tag{18}$$

where E_0 is the single-oscillator energy and E_d is the dispersion energy. By plotting $(n^2 - 1)^{-1}$ vs. $(h\nu)^2$ and fitting straight lines as shown in Fig. 5, E_0 and E_d can be determined from the intercept, E_0/E_d and the slope $(E_0 \cdot E_d)^{-1}$. Fig. 5 also shows the values of

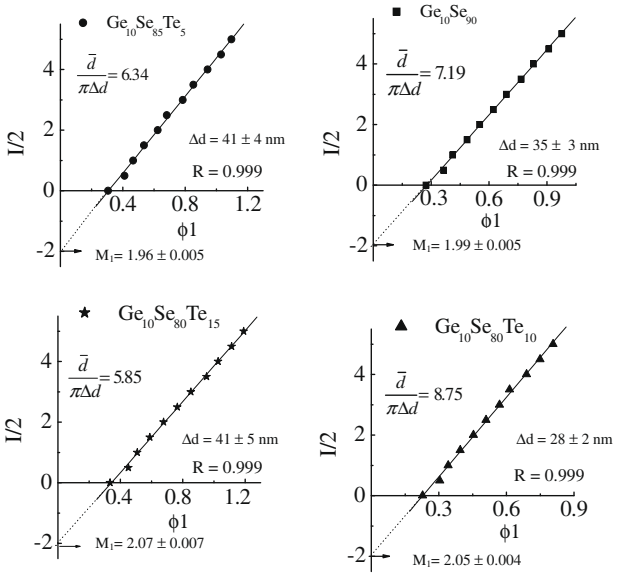

Fig. 3. The linear relation between l/2 and ϕ_1, in order to determine m_1 and Δd for $Ge_{10}Se_{90-x}Te_x$ thin films.

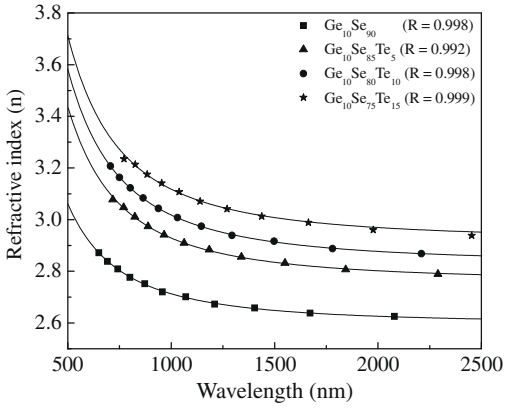

Fig. 4. Refractive index, n, as a function of, λ, for different compositions of $Ge_{10}Se_{90-x}Te_x$ thin films. Solid curves are determined according to the single-oscillator analysis.

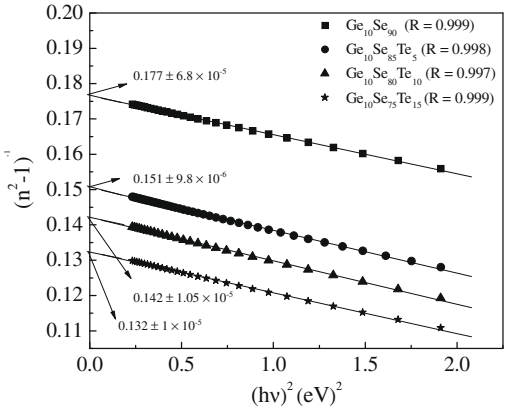

Fig. 5. Plots of refractive index factor $(n^2-1)^{-1}$ vs. $(h\nu)^2$ for different compositions of $Ge_{10}Se_{90-x}Te_x$ films.

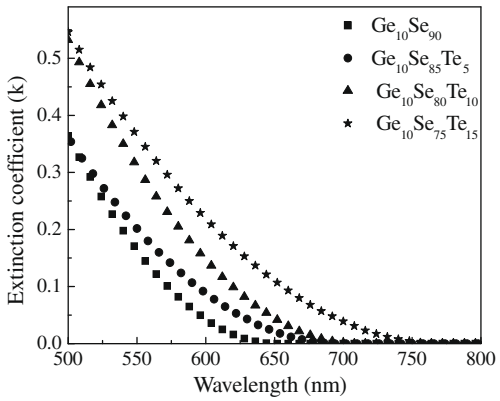

Fig. 6. Plots of the extinction coefficient, k, vs., λ, for $Ge_{10}Se_{90-x}Te_x$ thin films.

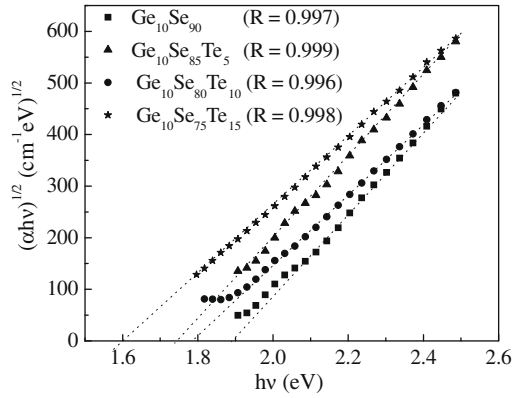

Fig. 7. The dependence of $(\alpha h\nu)^{1/2}$ on photon energy, $h\nu$, for the different composition of amorphous $Ge_{10}Se_{90-x}Te_x$ thin films from which the optical band gap, E_g, is estimated (Tauc extrapolation).

refractive index extrapolated to $h\nu = 0$ for four different composition samples.

As the procedure by Swanepoel [20] recommends for determining the extinction coefficient, k, or absorption coefficient (α) based on the above-mentioned optical dispersion relationship, which presented in Eq. (15). Then the extinction coefficient, k, as function of, λ, for $Ge_{10}Se_{90-x}Te_x$ thin films are shown in Fig. 6.

Fig. 7 shows the variation of $(\alpha h\nu)^{1/2}$ as a function of photon energy, $h\nu$, for $Ge_{10}Se_{90-x}Te_x$ thin films. For the higher values of the absorption coefficient ($\alpha > 10^4\ cm^{-1}$) the photon energy dependence of the absorption coefficient for the allowed non-direct transitions can be described by $(\alpha h\nu)^{1/2} = B(h\nu - E_g)$ where B is a parameter that depends on the transition probability and E_g is the optical energy gap [31,32].

5. Discussion

From Fig. 5 and Table 2 one can observed that, the single-oscillator energy, E_0, decreases, while the dispersion energy, E_d, and the refractive index, $n(0)$ increase with increasing Te content. E_0 is considered as an average energy gap to a good approximation related to the optical band gap, E_g, ($E_0 \approx 2E_g$) [32]. WDD model is related to the dispersion energy, E_d, and other physical parameters of material through the following empirical relationship [30]:

$$E_d = \beta \cdot N_c \cdot Z_a \cdot N_e \ (\mathrm{eV}), \tag{19}$$

where N_c is the effective coordination number of the cation nearest neighbors to the anion, Z_a is the formal chemical valency of the an-

Table 2
Optical band gap, E_g, Wemple–DiDomenico dispersion parameters (E_0 and E_d), E_0/E_g ratio, values of refractive index $n(0)$, the excess of Se–Se homopolar bonds and the cohesive energy, CE, for different compositions of $Ge_{10}Se_{90-x}Te_x$ thin film.

Composition	$E_g \pm 0.02$ (eV)	$E_0 \pm 0.02$ (eV)	$E_d \pm 0.4$ (eV)	E_0/E_g	$n(0) \pm 0.001$	Excess Se–Se	CE (eV atom^{-1})
$Ge_{10}Se_{90}$	1.90	3.99	22.59	2.1	2.16	140	59.1
$Ge_{10}Se_{85}Te_5$	1.78	3.53	23.36	1.98	2.37	120	56.9
$Ge_{10}Se_{80}Te_{10}$	1.75	3.4	23.92	1.94	2.46	100	54.8
$Ge_{10}Se_{75}Te_{15}$	1.61	3.38	25.56	2.09	2.56	80	52.6

ion, N_e is the effective number of valence electrons per anion, and β is a two-valued constant with the either an ionic or a covalent value ($\beta_i = 0.26 \pm 0.03$ eV and $\beta_c = 0.37 \pm 0.04$ eV, respectively). Therefore, in order to account for the compositional trended of E_d it is suggested that, the observed increase in E_d with increasing Te content is primarily due to the change in the ionicities (homopolar Se–Se bond are introduce together with the excess Se atoms that decreases with increasing Te content). The values of excess of Se–Se homopolar bonds for different compositions of $Ge_{10}Se_{90-x}Te_x$ thin films are listed in Table 2.

According to the chemical bond approach [33,34], bonds are formed in the sequence of decreasing bond energy until the available valence of atoms is satisfied. The bond energies $D(A-B)$ for heteronuclear bonds have been calculated by using the empirical relation

$$D(A-B) = [D(A-A)\cdot D(B-B)]^{1/2} + 30(\chi_A - \chi_B)^2 \quad (20)$$

proposed by Pauling [35], where $D(A-A)$ and $D(B-B)$ are the energies of the homonuclear bonds (kcal/mol.) [36], χ_A and χ_B are the electronegativity values for the involved atoms [33]. In the present compositions, the Ge–Se bonds with the highest possible energy (70.6 kcal mol^{-1}) are expected to occur firstly followed by Ge–Te bonds (49.2 kcal mol^{-1}) to saturate all available valence of Se. There are still unsatisfied Se which must be satisfied by forming Se–Se bonds. Based on the chemical bond approach, the bond energies are assumed to be additive. Thus, the cohesive energies were estimated by summing the bond energies over all the bonds expected in the material. Calculated values of the cohesive energies for all compositions are presented in Table 2. These results indicate that, the cohesive energies of these glasses show a decrease with increasing Te content. Therefore, it can be concluded that the decrease of E_g with increasing Te content (Table 2) is most probably due to the reduction of the average stabilization energy by increasing Te content. It should be mentioned that, the approach of the chemical bond neglects dangling bond and other valence defects as a first approximation. Also van der Walls interactions are neglected, which can provide a means for further stabilization by the formation of much weaker links than regular covalent bonds.

6. Conclusions

The suggested method by Swanepoel and Marquez is successfully applied to Ge–Se–Te semiconducting glassy films with non-uniform thickness. In the present study the problem of the optical characterization of wedge-shaped thin films is analyzed from both the theoretical and experimental points of view for characterizing Ge–Se–Te thin films using only the transmission spectrum at normal incidence. The formulae for the envelopes of the interference maxima and minima of the transmission spectrum are derived under the assumption that the thickness of the film investigated is not uniform. Furthermore, it is shown that the values of these envelopes are related to the values of the envelopes of the interference maxima and minima of the corresponding layer, with the uniform thickness equal to the average thickness of the wedge-shaped thin film. Thus, the values of the envelopes of the extreme of the uniform film mentioned can be determined using the values of the envelopes of the extreme of the wedge-shaped film that can be measured. These values are used for calculating the spectral dependences of the optical constants of the chalcogenide films investigated. The paper also describes the determination of the average thickness and the variation in thickness from this average thickness. It was found that, both of the optical band gap, E_g, and the single-oscillator energy, E_0, decrease while the refractive index and dispersion energy, E_d, increase by increasing Te content. The allowed non-direct electronic transition is mainly responsible for the photon absorption inside the investigated films. Further more, the subsequent fitting of the refractive indices to the single-oscillator model (Wemple–DiDomenico relationship) results in dispersion parameters directly related to the structure of the glassy material under study. Finally, the chemical bond approach has been applied successfully to interpret the decrease of the glass optical gap, E_g, with increasing Te content.

Acknowledgments

The author thanks Al-Azhar University for the financial support and Dr A. Dahshan, Department of Physics, Faculty of Science, Suez Canal University, Port Said, Egypt for his help and advice throughout this work.

References

[1] E . Marquez, J.M. Gonzalez-Leal, R. Jimenez-Garay, M . Vlcek, Thin Solid Films 396 (2001) 183.
[2] A. Vasko, in: Proceedings of the 11th International Congress on Glass, vol. 5, 1977, p. 533.
[3] J.A. Savage, Infrared Optical Materials and Their Antireflection Coatings, Adam Hilger, Bristol, 1985.
[4] S.M. El-Sayed, G.A.M. Amin, Vacuum 62 (2001) 353.
[5] S.A. Fayek, Mater. Chem. Phys. 62 (2000) 95.
[6] Pankaj Sharma, S.C. Katyal, Mater. Lett. 61 (2007) 4516.
[7] Pankaj Sharma, S.C. Katyal, Thin Solid Films 515 (2007) 7966.
[8] Shelly Jain, Sanjeev Gautam, D.K. Shukla, Navdeep Goyal, Appl. Surf. Sci. 147 (1999) 19.
[9] R. Ganesan, K.N. Madhusoodanan, A. Srinivasan, K.S. Sangunnil, E.S.R. Gopal, Phys. Stat. Sol. (b) 212, 223 (1999).
[10] A. El-Korashy, A. Bakry, M.A. Abdel-Rahim, M. Abd El-Sattar, Physica B 391 (2007) 266.
[11] S.A. Khan, M. Zulfequar, M. Husain, Physica B 324 (2002) 336.
[12] J. Tauc, Amorphous and Liquid Semiconductors, Plenum, New York, 1974.
[13] Z. Cimpl, F. Kosek, Phys. Stat. Sol. a 93 (1986) K55.
[14] D.A. Minkov, E. Vateva, E. Skordeva, D. Arsova, M. Niki-forova, J. Non-Cryst. Solids 90 (1987) 481.
[15] K.A. Aly, A.M. Abousehly, M.A. Osman, A.A. Othman, Physica B 403 (2008) 1848.
[16] L. Vriens, W. Rippens, Appl. Opt. 22 (1983) 4105.
[17] D.P. Arndt, R.M.A. Azzam, J.M. Bennett, J.P. Borgogno, C.K. Carniglia, W.E. Case, J.A. Dobrowolski, U.J. Gibson, T. Tuttle Hart, F.C. Ho, V.A. Hodgkin, W.P. Klapp, H.A. Macleod, E. Pelletier, M.K. Purvis, D.M. Quinn, D.H. Strome, R. Swenson, P.A. Temple, T.F. Thonn, Appl. Opt. 23 (1984) 3571.
[18] D.A. Minkov, J. Mod. Opt. 37 (1990) 1977.
[19] R. Swanepoel, J. Phys. E I6 (1983) 1214.
[20] R. Swanepoel, J. Phys. E: Sci. Instrum. 17 (1984) 896.
[21] E. Màrquez, J. Ramirez-Malo, P. Villares, R. Jimenez-Garay, P.J.S. Ewen, A.E. Owen, J. Phys. D 25 (1992) 535.
[22] R. Glang, Handbook of Thin Film Technology, McGraw-Hill, New York, 1983.
[23] A. Dahshan, K.A. Aly, Acta Mater. 56 (2008) 4869.
[24] A. Dahshan, H.H. Amer, K.A. Aly, J. Phys. D: Appl. Phys. 41 (2008) 215401.

[25] J.M. Gonzàlez-Leal, M. Stuchlik, M. Vlcek, R. Jimènez-Garay, E. Màrquez, Appl. Surf. Sci. 246 (2005) 348.
[26] J.M. Gonzàlez-Leal, R. Prieto-Alcón, M. Vlcek, E. Màrquez, J. Non-Cryst. Solids 345&346 (2004) 88.
[27] O.S. Heavens, Optical Properties of Thin Solid Films, Butterworths, London, 1955.
[28] J.B. Ramirez-Malo, E. Màrquez, P. Villares, R. Jimenez-Garay, Mater. Lett. 17 (1993) 327.
[29] T.S. Moss, Optical Properties of Semiconductors, Butterworths, London, 1959.
[30] S.H. Wemple, M. DiDomenico, Phys. Rev. B 3 (1971) 1338.
[31] E.A. Davis, N.F. Mott, Philos. Mag. 22 (1970) 903.
[32] K. Tanaka, Thin Solid Films 66 (1980) 271.
[33] J. Bicermo, S.R. Ovshinsky, J. Non-Cryst. Solids 74 (1985) 75.
[34] B. Jozef, O. Stanford, S. Mahadevan, A. Gridhar, A.K. Singh, J. Non-Cryst. Solids 74 (1985) 75.
[35] J. Pauling, Nature of the Chemical Bond Ithaca, Cornell University, NY, 1960.
[36] L. Tichy, A. Triska, H. Ticha, M. Frumar, J. Klikorka, Solid State Commun. 41 (1982) 751.